Supplementary Information

Electrocatalysis hydrogen evolution using MS_2@MoS_2/RGO (M=Fe or Ni) hybrid catalyst

Yaxiao Guo,[a,b] Changshuai Shang,[a,b] Xiaoyan Zhang[a,b] and Erkang Wang[a*]

[a] State Key Laboratory of Electroanalytical Chemistry, Changchun Institute of Applied Chemistry, Chinese Academy of Sciences, 5625 Renmin Street, Changchun, Jilin 130022, China. E-mail: ekwang@ciac.ac.cn

[b] University of Chinese Academy of Sciences, 19A Yuquan Road, Beijing, 100049, China.

Experimental Section

Materials and Reagents

Ferrous chloride tetrahydrate, nickel nitrate hexahydrate, phosphomolybdic acid hydrate (PMA), L-cysteine, nafion solution (5 wt%) and graphite rod (99.9995%) were purchased from Sigma-Aldrich. Absolute ethanol, sulphuric acid (H_2SO_4, 95.0-98.0%), hydrochloric acid (HCl, 36.0-38.0%), hydrogen peroxide (H_2O_2, 30.0%), potassium persulfate ($K_2S_2O_8$), phosphorus pentoxide (P_2O_5), sodium nitrate ($NaNO_3$) and potassium permanganate ($KMnO_4$) were obtained from Beijing Chemical Co. (China). The ultra-pure water was prepared by the Millipore Milli-Q water purification system (18.2 MΩ). All reagents were used directly without further purification.

Materials synthesis

Synthesis of Graphene Oxide (GO). GO was made by a modified Hummers method.[1] The detailed procedure was described as follows. (1) **Preoxidation**: To a stirred solution of concentrated H_2SO_4 (15 mL) were added $K_2S_2O_8$ (5 g) and P_2O_5 (5 g) in turn. Then the solution was heated to 80 ^oC before graphite (1 g) was added. The resulting mixture was stirred for 6 h at 80 ^oC and cooled to room temperature by injecting 100 mL ultra-pure water. Subsequently, the suspension was centrifuged and rinsed with a large amount of ultra-pure water repeatedly until the pH reached ~ 7. At last, the residue was dried at vacuum to obtain the product of preoxidation. (2) **Peroxidation**: In a three-neck round bottom flask was added concentrated H_2SO_4 (23 mL) and cooled to 0 ^oC using an ice salt bath before the product of preoxidation and $NaNO_3$ (0.5 g) were added. Then $KMnO_4$ (3 g) was slowly added to the flask and the resulting solution was stirred at 35 ^oC for 2 h. Water (46 mL) was added and the mixture was heated to 85 ^oC and stirred at this temperature for 15 minutes. Afterwards, water (140 mL) and 30% H_2O_2 (10 mL) were added into the flask to terminate the reaction. The suspension was centrifuged before the residue was washed with 5% HCl solution twice and further rinsed with a large amount of water repeatedly. Then the residue was dispersed in 500 mL of water and dialysed for 7 days. Finally, GO was obtained by centrifuging and drying under vacuum.

Preparation of MS_2@MoS_2/rGO (M = Fe or Ni) hybrid. The fabrication process for the MS_2@MoS_2/rGO (M = Fe or Ni) hybrid is illustrated in Scheme 1. Firstly, 0.15 mM PMA was dissolved into 22.5 ml GO solution (1 mg/ml) with stirring at room temperature for 30 min. Then, L-cysteine (S:Mo=4:1) was dissolved into and stirred for 30 minutes. Finally Fe or Ni precursor (M:Mo=1:1, M=Fe or Ni) were dissolved into. The mixture was stirred at room temperature until a homogeneous solution was achieved before transferred to a 30 mL Teflon-lined autoclave. It was heated in an oven at 200°C for 12 h with no intentional control of ramping or cooling rate. The final product was collected by centrifugation at 10000 rpm for 10 min, and

washed with ultra-pure water and absolute ethanol for several times to remove any possible ions. Finally, product was frozen by liquid nitrogen and lyophilized for 24 h. MoS_2/rGO was prepared with the same procedure in the absence of Fe (or Ni) precursor. MoS_2 was prepared in the absence of GO and Fe (or Ni) precursor.

Characterizations

The morphology of different materials is observed with scanning electron microscopy (SEM, PHILIPS XL-30 ESEM) operated at the accelerating voltage of 20 kV. Transmission electron microscopy (TEM), high-resolution TEM (HRTEM), high-angle annular dark field (HAADF)-scanning transmission electron microscopy (STEM), and STEM-energy dispersive X-ray (EDX) mapping were taken by using a JEM-2010 (HR) microscope operated at an accelerating voltage 200 kV. The X-ray diffraction (XRD) patterns of samples were recorded on a Bruker D8 ADVANCE instrument with Cu Kα radiation (40 kV, 40 mA). The X-ray photoelectron spectroscopy (XPS) was collected by a Thermo ESCALAB 250 with Al Kα radiation (pass energy, 20.0 eV; energy step size. 1.0 eV; total acq. time: 1 min 0.1 s). Raman spectra are measured and collected using Renishaw RM-1000 with a laser excitation of 514.5 nm. The Nyquist plots (EIS) were performed on Zahner Zennium. All electrochemical measurements were performed on CHI620a.

Electrochemical Measurements

The electrochemical experiments for HER were carried out with an electrochemical workstation (CHI620a) at room temperature using a three-electrode configuration with the glassy carbon electrode with various samples, Ag/AgCl (saturated KCl) electrode and a graphite rod as working electrode, reference electrode and counter electrode, respectively. The preparation of the working electrode is similar to the reference.[2] Typically, 4 mg of sample and 30 μL Nafion solution (5 wt%) were dispersed in 1 mL water-ethanol solution with volume ratio of 3:1 by sonicating to form a homogeneous ink. Then 5 μL of the dispersion (containing 20 μg of catalyst) was loaded onto a glassy carbon electrode of 3 mm diameter (loading ca. 0.285 mg cm^{-2}). For comparison, we also performed measurements using a commercial Pt catalyst (20 wt% Pt on Vulcan carbon black) exhibiting high HER catalytic performance. The polarization curves were obtained in 0.5 M H_2SO_4 (sparged with pure N_2) with a scan rate of 5 mV s^{-1} at room temperature. All of the potentials were iR-compensated and converted to a reversible hydrogen electrode (RHE) scale via calibration according to the literature.[3] In 0.5 M H_2SO_4, $E_{RHE}=E_{Ag/AgCl}+0.217$ V. All the potentials reported in our manuscript were against RHE. And the presented current density was normalized to the geometric surface area. All the polarization curves are the steady-state ones after several cycles.

The ohmic resistance used for iR-compensated was obtained from electrochemical impedance spectroscopy (EIS) measurements with frequencies ranging from 100 mHz

to 1M Hz with an AC voltage of 5 mV. The impedance data were fitted to a simplified Randles circuit to extract the series resistances (R_s) and charge-transfer resistances (R_{ct}).

The electrochemical stability of different catalysts was evaluated by CV from +0.10 V to −0.4V vs. RHE with a scan rate of 50 mV s^{-1}, cycling the electrode 1000 times. Amperometric i-t curve was also obtained at a constant potential of -0.15 V vs. RHE to evaluate the stability.

The electrochemical double layer capacitances (C_{dl}) were measured to evaluate the effective surface area of various catalysts. A potential range of 0.1-0.2 V vs. RHE is selected for the capacitance measurements. This is due to the fact that no obvious Faradic current was observed in this region for each catalyst. The capacitive currents of $\Delta j_{0.15V}/2$ are plotted as a function of the CV scan rate of 20-200 mV s^{-1}. The slope of the line fitted by these data is the geometric C_{dl}.

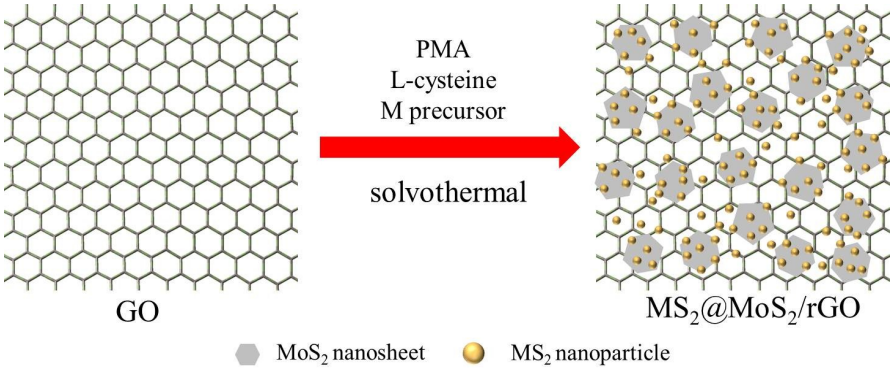

Scheme S1. The fabrication process of the MS_2@MoS_2/rGO (M = Fe or Ni).

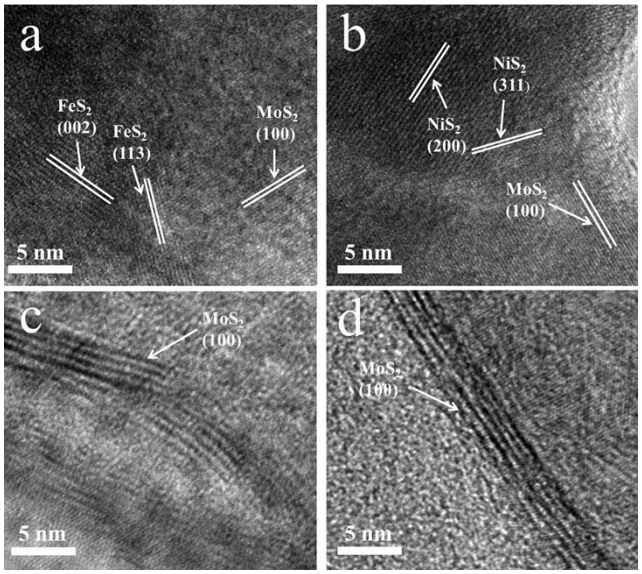

Fig. S1. HRTEM images of (a, c) FeS_2@MoS_2/rGO and (b, d) NiS_2@MoS_2/rGO.

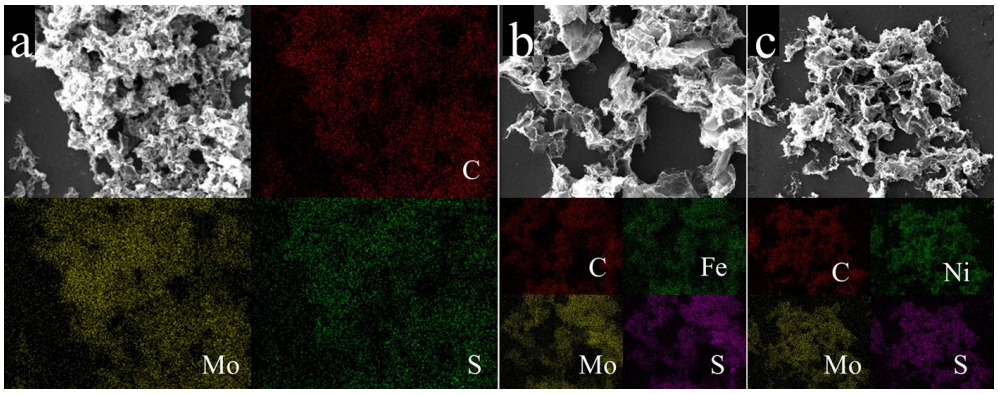

Fig. S2. STEM and EDS mapping images of (a) MoS_2/rGO, (b) FeS_2@MoS_2/rGO and (c) NiS_2@MoS_2/rGO.

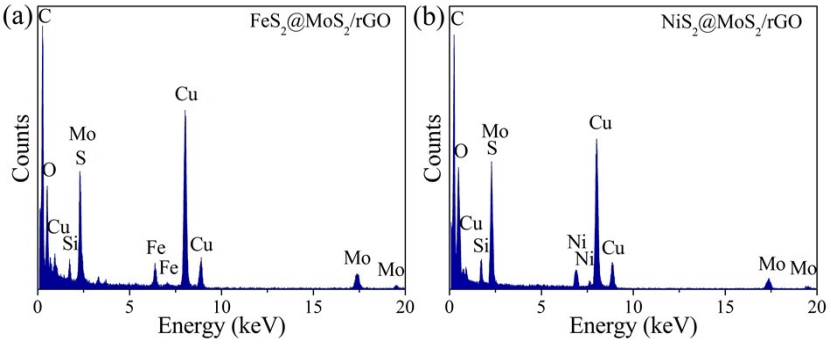

Fig. S3. Energy dispersive X-ray (EDX) spectra of (a) FeS_2@MoS_2/rGO and (b) NiS_2@MoS_2/rGO.

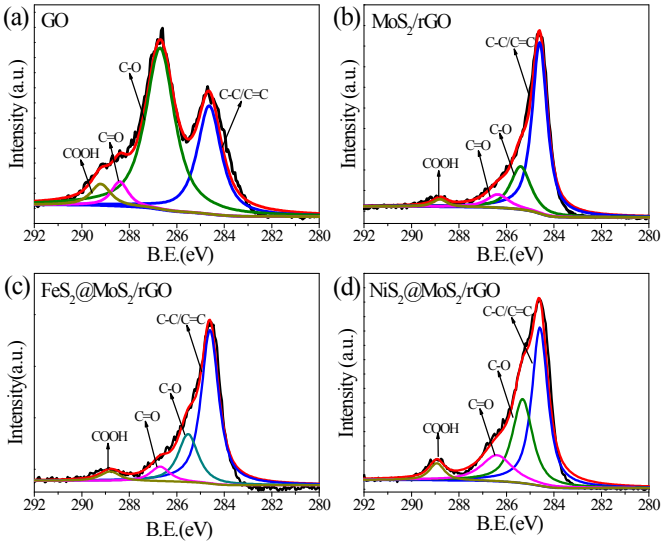

Fig. S4. The C 1s XPS spectra of (a) GO, (b) MoS_2/rGO, (c) FeS_2@MoS_2/rGO and (d) NiS_2@MoS_2/rGO.

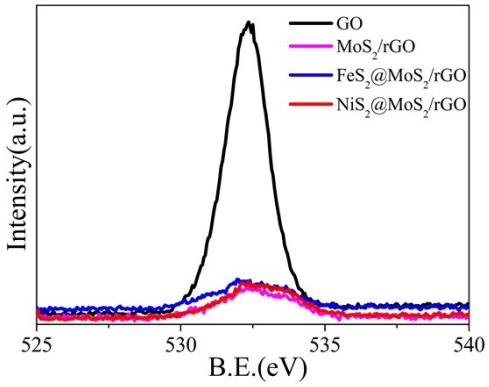

Fig. S5. The O 1s XPS spectra of (a) GO, (b) MoS_2/rGO, (c) FeS_2@MoS_2/rGO and (d) NiS_2@MoS_2/rGO.

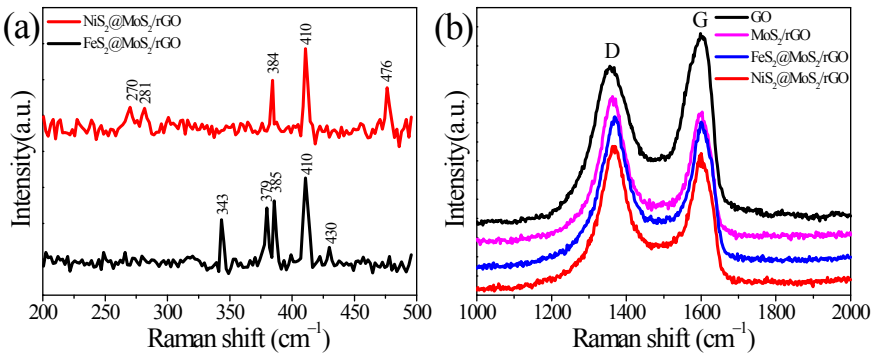

Fig. S6. Raman spectra of FeS_2@MoS_2/rGO and NiS_2@MoS_2/rGO.

Table S1. Electrochemical parameters of different materials.

Materials	$\eta_{j=10}$ [a]	$\eta_{j=100}$ [b]	b [c]	j_0 [d]	C_{dl} [e]	R_{ct} [f]
MoS_2	318	---	94.1	4.1	4.8	191.3
MoS_2/rGO	161	285	52.4	11.6	10.7	1.5
FeS_2@MoS_2/rGO	123	224	38.4	17.5	19.0	1.3
NiS_2@MoS_2/rGO	110	202	38.5	19.6	21.4	1.2

[a] Overpotential (mV) at current density of 10 mA cm^{-2}. [b] Overpotential (mV) at current density of 100 mA cm^{-2}. [c] Tafel slope (mV dec^{-1}). [d] Exchange current density (μA cm^{-2}). [e] Double-layer capacitance (mF cm^{-2}). [f] The charge transfer resistances (Ω).

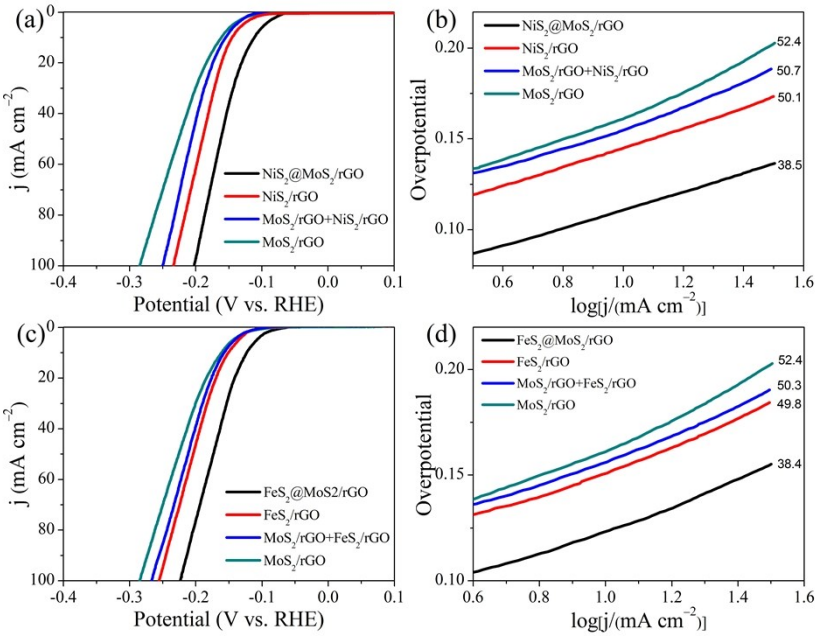

Fig. S7 LSV curves and Tafel plots of MoS_2/RGO+NiS_2/RGO (a and b), MoS_2/RGO+FeS_2/RGO (c and d).

Table S2. Electrochemical parameters of different catalysts.

Catalyst	Mass loading [mg cm^{-2}]	Tafel slopes [mV dec^{-1}]	$\eta_{j=10}$ [mV]	$\eta_{j=100}$ [mV]
MoS_2⊥RGO[4]	0.204	43	172	Not given
FeCo@NCNTs-NH[5]	0.32	74	Not given	Not given

			(~280 mV by estimating)	
Defect-rich MoS_2 nanosheets[6]	0.285	50	Not given (~190 mV by estimating)	Not given
CoNi@NC[7]	0.32	104	224	Not given
MoS_2/RGO[8]	0.280	41	Not given (~150 mV by estimating)	Not given
Oxygen-incorporated MoS_2 nanosheets[9]	0.285	55	Not given (~180 mV by estimating)	Not given (~280 mV by estimating)
MoS_2 nanosheets within graphite[10]	0.200	41	Not given (~160 mV by estimating)	Not given (~280 mV by estimating)
$Fe_{0.9}Co_{0.1}S_2$/CNT[11]	7.0	46	Not given (~120 mV at 20 mA cm^{-2} by estimating)	170
NiS_2@MoS_2/rGO (current work)	0.285	38.5	110	202
FeS_2@MoS_2/rGO (current work)	0.285	38.4	123	224

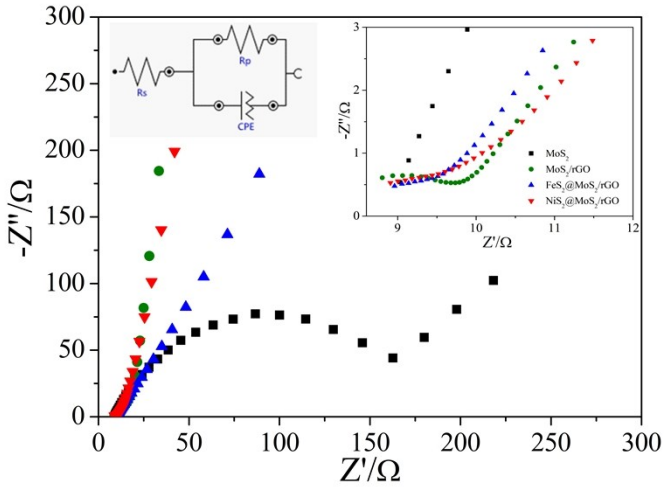

Fig. S8. Nyquist plots of different materials in this work (a), the magnified image zoomed from (a).

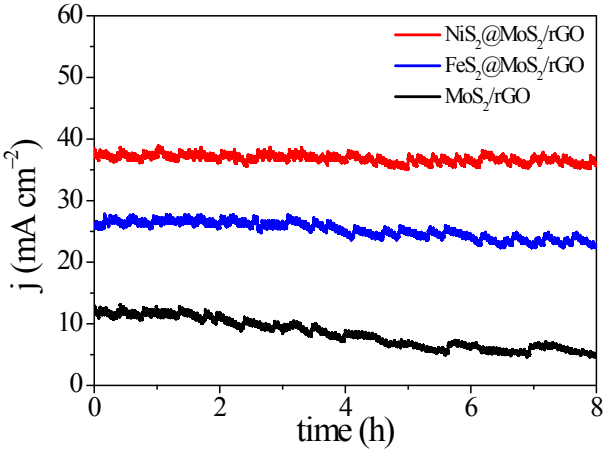

Fig. S9. Current versus time during the long term (8 h) with a constant potential (− 0.15 V vs. RHE).

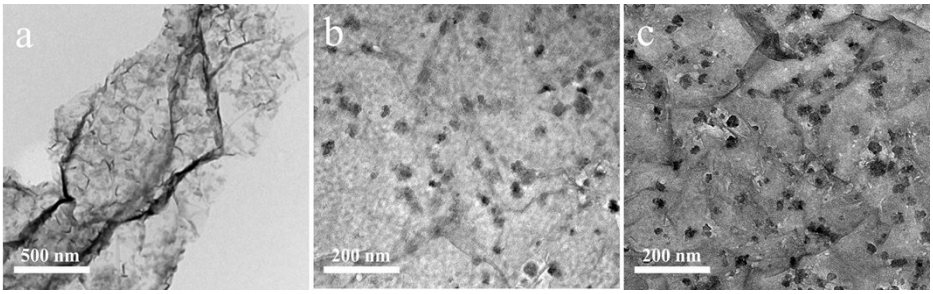

Fig. S10. TEM images of (a) MoS_2/rGO, (b) FeS_2@MoS_2/rGO and (c) NiS_2@MoS_2/rGO after the stability test (8 h)

References

1. S. Hou, M. L. Kasner, S. Su, K. Patel and R. Cuellari, *J. Phys. Chem. C*, 2010, **114**, 14915.
2. J. Xie, H. Zhang, S. Li, R. Wang, X. Sun, M. Zhou, J. Zhou, X. W. Lou and Y. Xie, *Adv. Mater*., 2013, **25**, 5807.
3. Y. Li, H. Wang, L. Xie, Y. Liang, G. Hong and H. Dai, *J. Am. Chem. Soc*., 2011, **133**, 7296.
4. Z. H. Deng, L. Li, W. Ding, K. Xiong and Z. D. Wei. *Chem. Commun*. 2015, **51,** 1893.
5. J. Deng, P. Ren, D. Deng, L. Yu, F. Yang and X. Bao. *Energy Environ. Sci*. 2014, **7**, 1919.
6. J. Xie, H. Zhang, S. Li, R. Wang, X. Sun, M. Zhou, J. Zhou, X. W. Lou and Y. Xie, *Adv. Mater*. 2013, **25**, 5807.
7. J. Deng, P. Ren, D. Deng and X. Bao, *Angew. Chem. Int. Ed*. 2015, **54**, 2100.
8. Y. Li, H. Wang, L. Xie, Y. Liang, G. Hong and H. Dai, *J. Am. Chem. Soc*. 2011, **133**, 7296.
9. J. Xie, J. Zhang, S. Li, F. Grote, X. Zhang, H. Zhang, R. Wang, Y. Lei, B. Pan and Y. Xie, *J. Am. Chem. Soc*. 2013, **135**, 17881.
10. X. Zheng, J. Xu, K. Yan, H. Wang, Z. Wang and S. Yang, *Chem. Mater*. 2014, **26**, 2344.
11. D.-Y. Wang, M. Gong, H.-L. Chou, C.-J. Pan, H.-A. Chen, Y. Wu, M.-C. Lin, M. Guan, J. Yang, C.-W. Chen, Y.-L. Wang, B.-J. Hwang, C.-C. Chen and H. Dai, *J. Am. Chem. Soc*. 2015, **137**, 1587.